Electronic Supplementary Material (ESI) for New Journal of Chemistry.
This journal is © The Royal Society of Chemistry and the Centre National de la Recherche Scientifique 2018

Supporting Information

IClick cycloaddition reaction of light-triggered manganese(I) carbonyl complexes

Ahmed M. Mansour, [a,b]*, and Alexandra Friedrich [b]

[a] Department of Chemistry, Faculty of Science, Cairo University,

Gamma Street, Giza, Cairo 12613, Egypt

[b] Institut für Anorganische Chemie, Julius-Maximilians-Universität Würzburg,

Am Hubland, D-97074 Würzburg, Germany

* mansour@sci.cu.edu.eg;

ahmed.mansour@uni-wuerzburg.de

* Corresponding author

Synthetic procedures

Synthesis of benzimidazole ligands

L^{SO3H} [19]

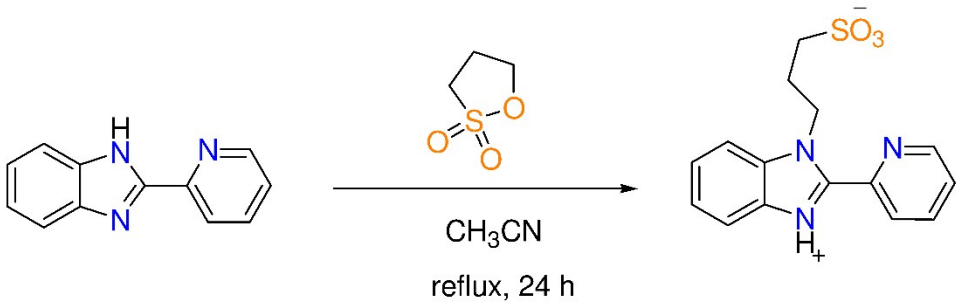

To an acetonitrile solution (50 mL) of 2-(2-pyridyl)benzimidazole (0.95 g, 5 mmol), 1.83 g of 1,3-propane sultone (15 mmol) was added and the reaction mixture was heated to reflux under argon for 24 h, whereupon a white precipitate was formed. The precipitate was collected by filtration, washed with acetonitrile and diethyl ether and dried *in vacuo*.

L^{PPH3} [19]

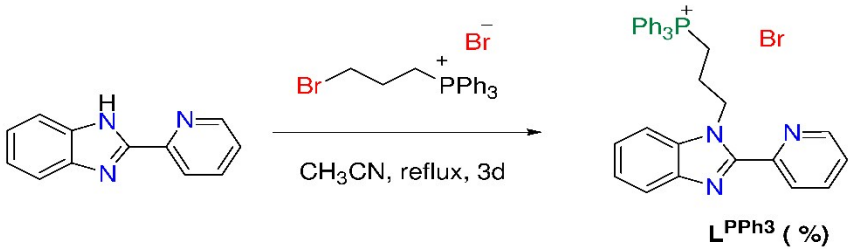

1-Bromopropyl-3-triphenylphosphonium bromide (2.33 g, 5 mmol) was added to the acetonitrile (50 mL) of 2-(2-pyridyl)benzimidazole (0.95 g, 5 mmol) and the resulting reaction mixture was heated to reflux for three days, whereupon a pale yellow precipitate was formed during the evaporation of the solution. The ligand was collected by filtration, washed with diethyl ether and dried in *vacuo*.

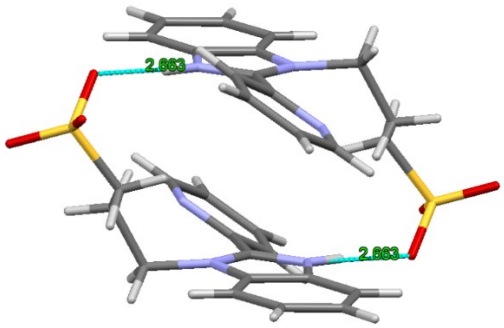

Fig. S1: Intermolecular H-bonding stabilizing the crystal packing of ligand L^{SO3H}.

Table S1: X-ray crystallographic data for $\mathbf{L^{SO3H}}$ and **2** at 100 K		
	$\mathbf{L^{SO3H}}$	**2**
formula	$C_{15}H_{15}N_3O_3S$	$C_{36}H_{29}BrMnN_3O_3P$, $0.5(C_6H_{14})$, Br
formula weight (g mol^{-1})	317.36	840.44
crystal system	Monoclinic	Triclinic
space group	$P2_1/n$	$P\ \bar{1}$
dimensions, mm^3	0.166×0.324×0.324	0.348×0.349×0.577
a, Å	10.900(4)	11.095(4)
b, Å	10.922(5)	13.234(4)
c, Å	11.836(5)	14.057(7)
α, deg	90	87.477(15)
β, deg	94.186(18)	88.554(19)
γ, deg	90	87.35(2)
V, Å^3	1405.3(10)	2059.3(13)
Z	4	2
ρ_{calcd}, g cm^{-3}	1.500	1.355
μ, mm^{-1}	0.248	2.336
θ range, deg	2.453 to 26.021°	2.071 to 26.022°
completeness to θ, %	100	100
reflections (all)	12415	34872
reflections (gt)	2772	8121
restraints	0	61
parameters	199	474
R(all)	0.0521	0.0485
R(gt)	0.0390	0.0400
wR(ref)	0.0956	0.1032
wR(gt)	0.0880	0.0997
goodness of fit (F^2)	1.040	1.037
Max/min residual electron density, e/Å^3	0.369 / –0.309	1.121 / –0.879

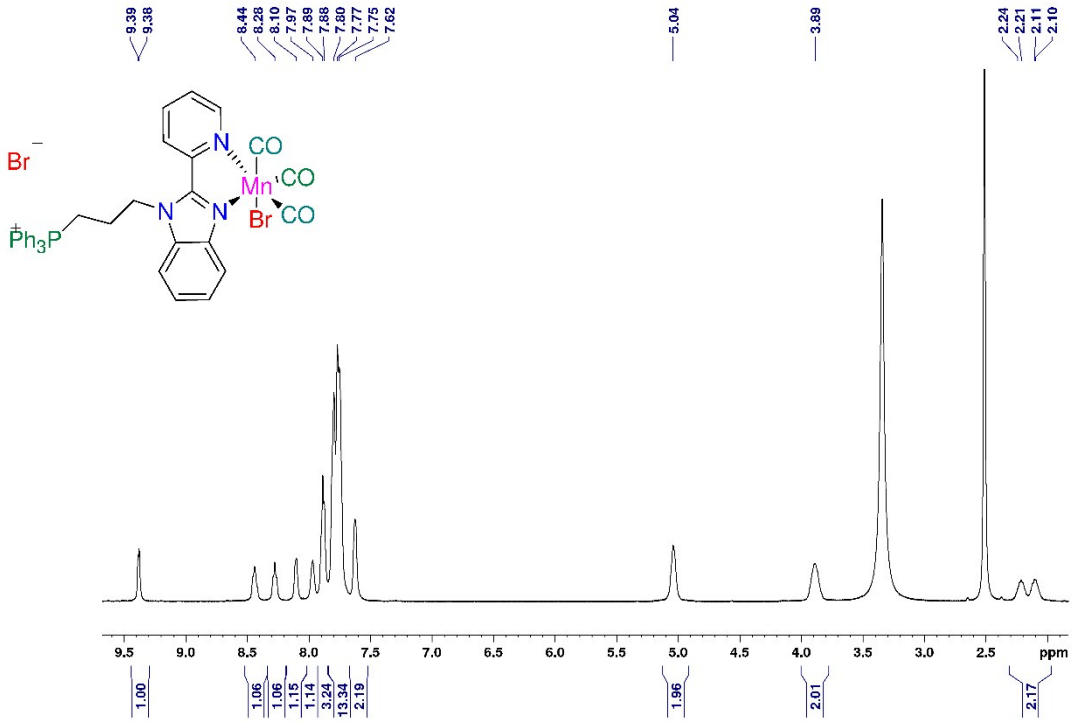

a)

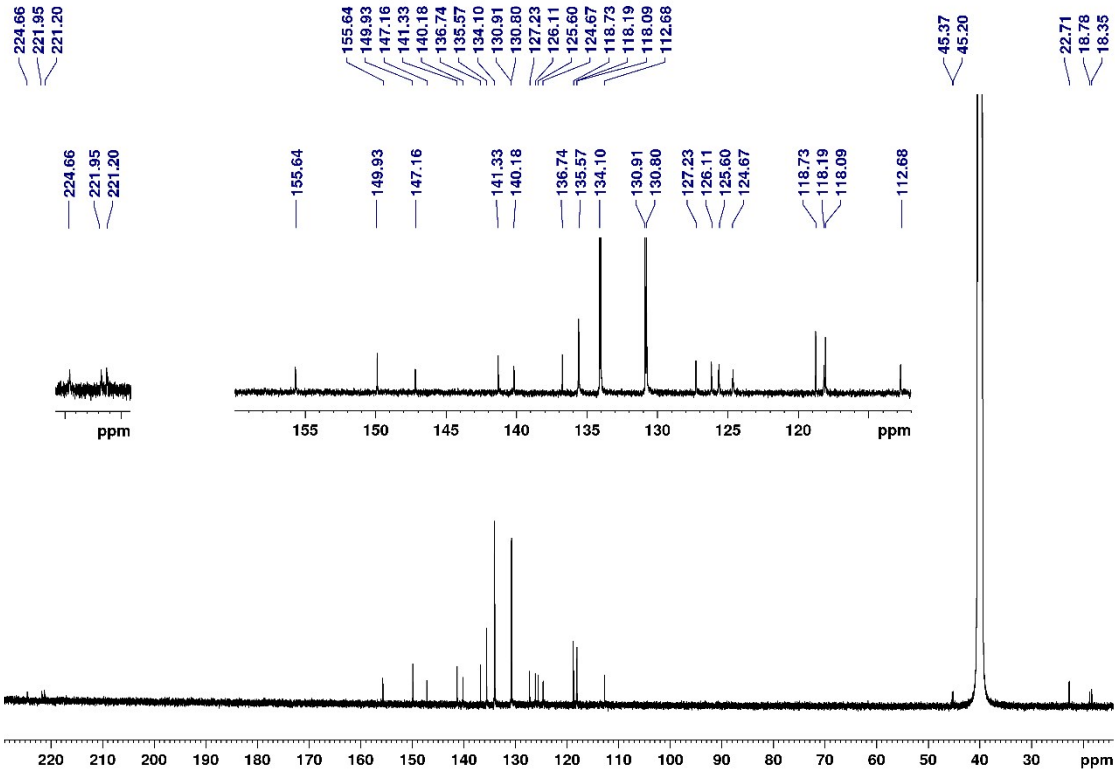

b)

Fig. S2: NMR analysis of **2** in DMSO-d_6, a) ^{1}H and b) ^{13}C spectra.

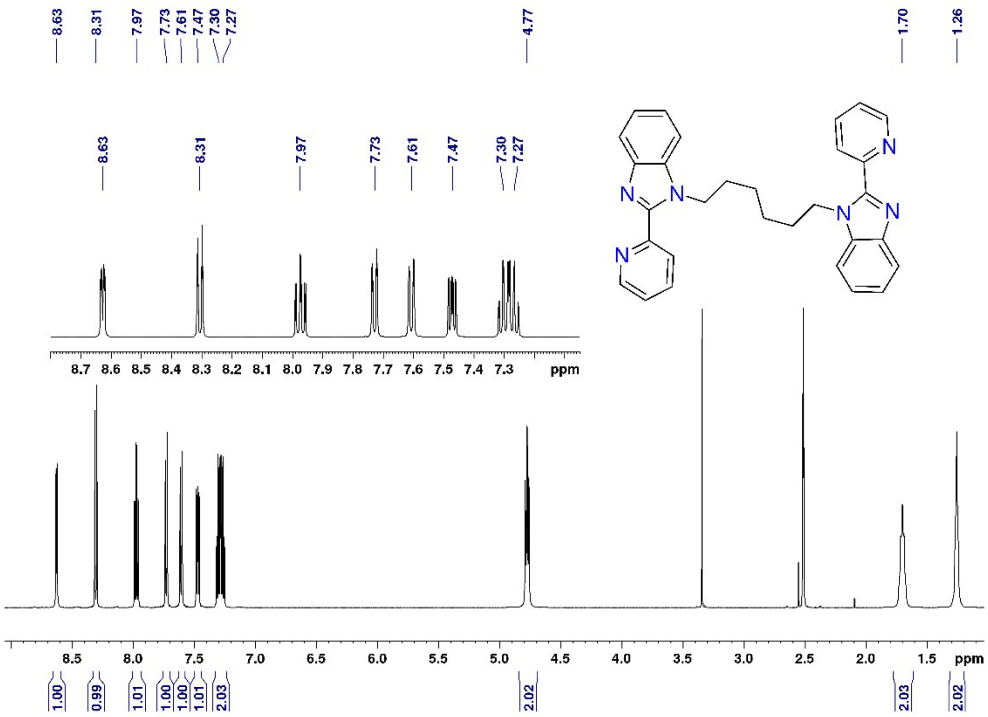

a)

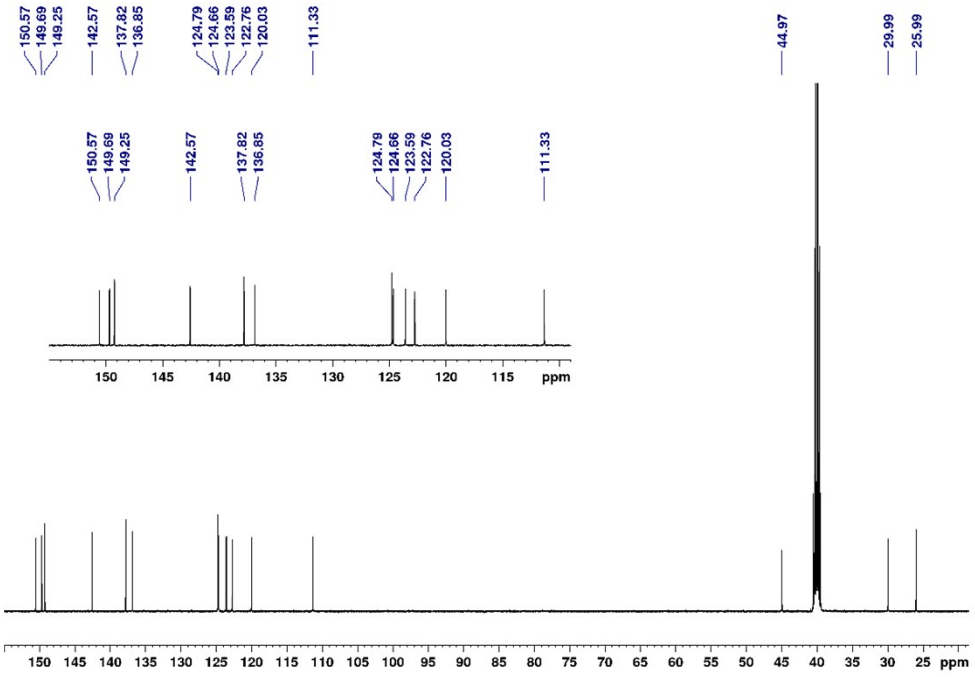

b)

Fig. S3: NMR analysis of L^{BPY} in DMSO-d_6, a) ^{1}H, and b) ^{13}C spectra.

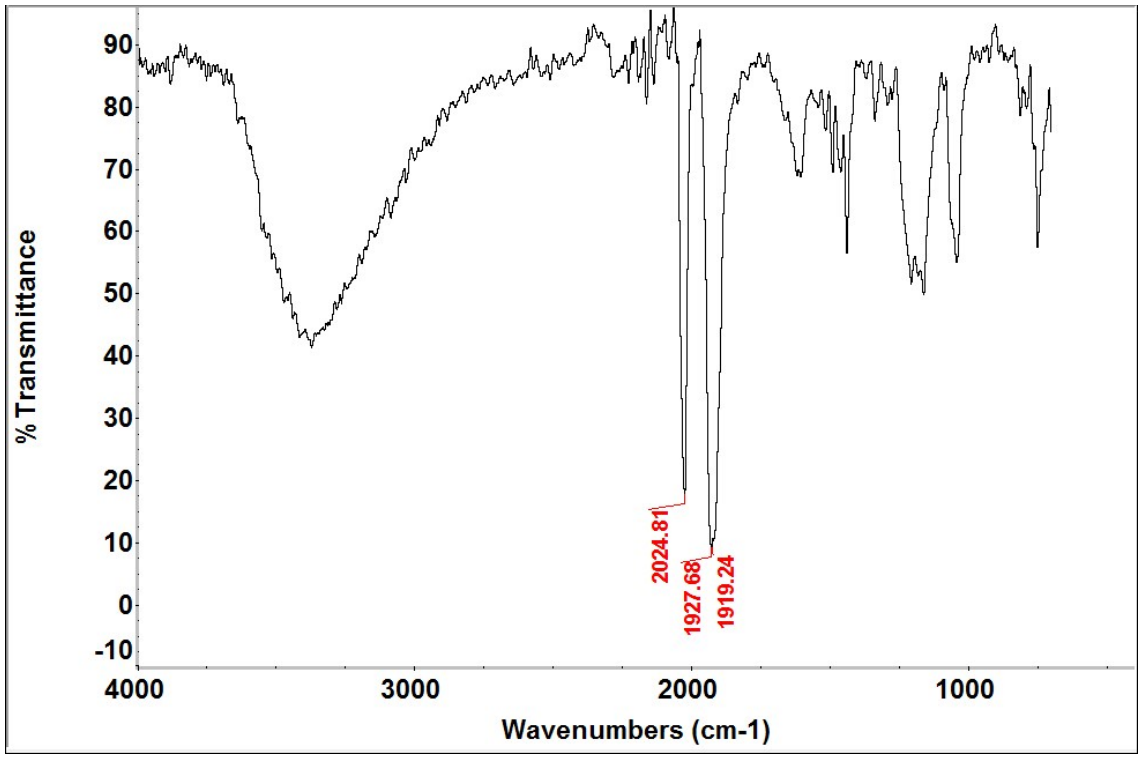
% Transmittance
90
80
70
60
50
40
30
20
10
0
-10
4000
3000
2000
1000
Wavenumbers (cm-1)
2024.81
1927.68
1919.24

a)

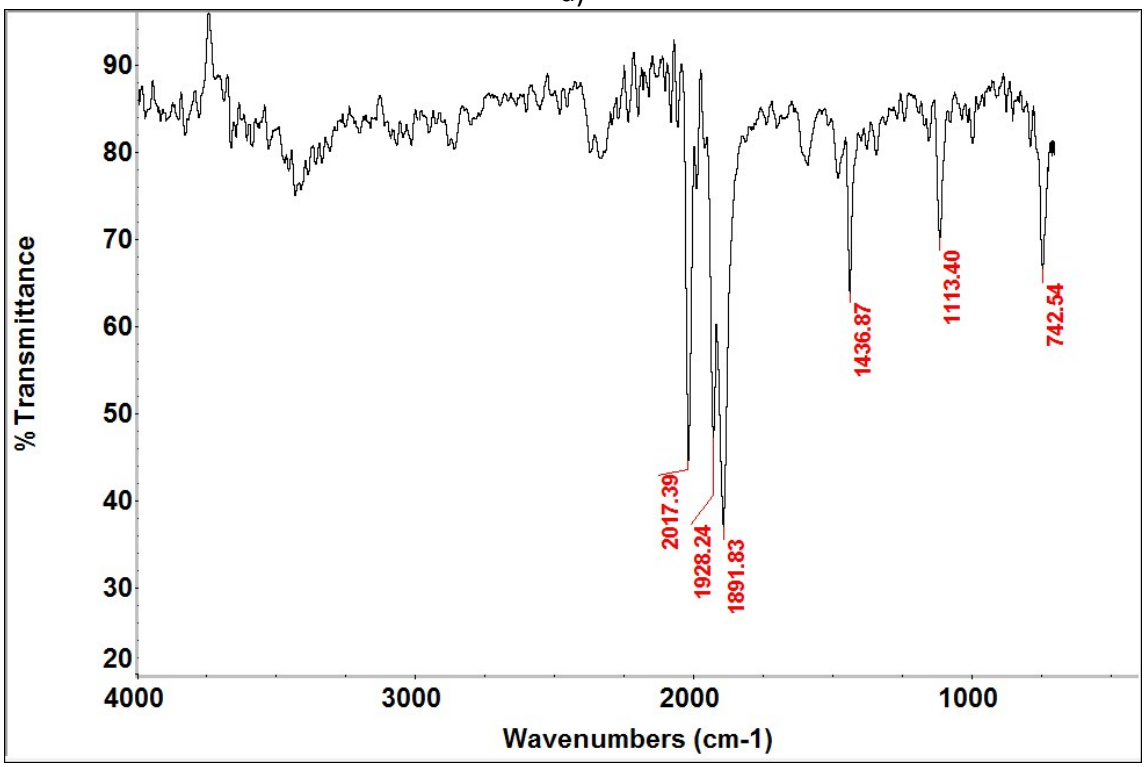
% Transmittance
90
80
70
60
50
40
30
20
4000
3000
2000
1000
Wavenumbers (cm-1)
2017.39
1928.24
1891.83
1436.87
1113.40
742.54

b)

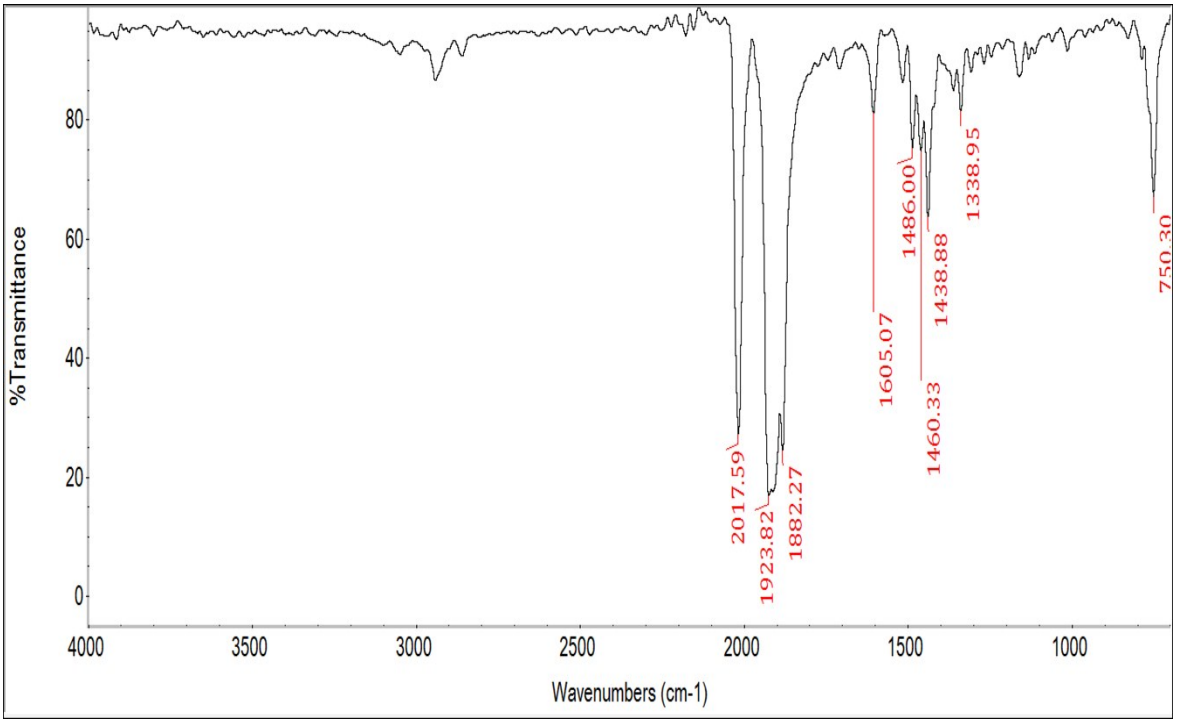

c)

Fig. S4: AT IR spectra of a) **1**, b) **2,** and c) **3**.

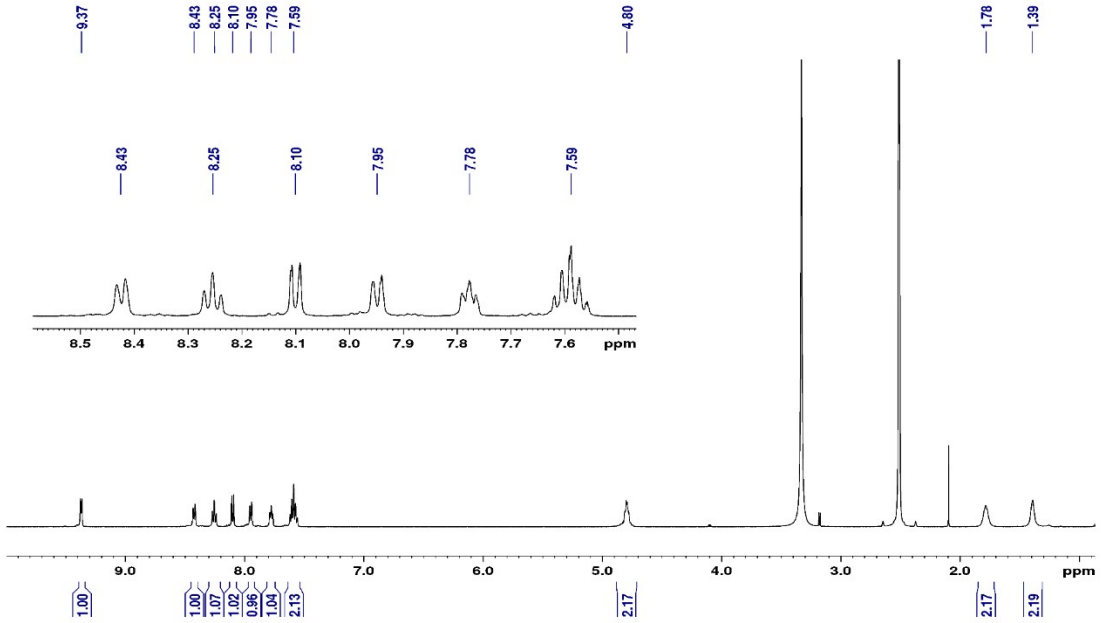
9.37
8.43
8.25
8.10
7.95
7.78
7.59
4.80
1.78
1.39
ppm

a)

b)

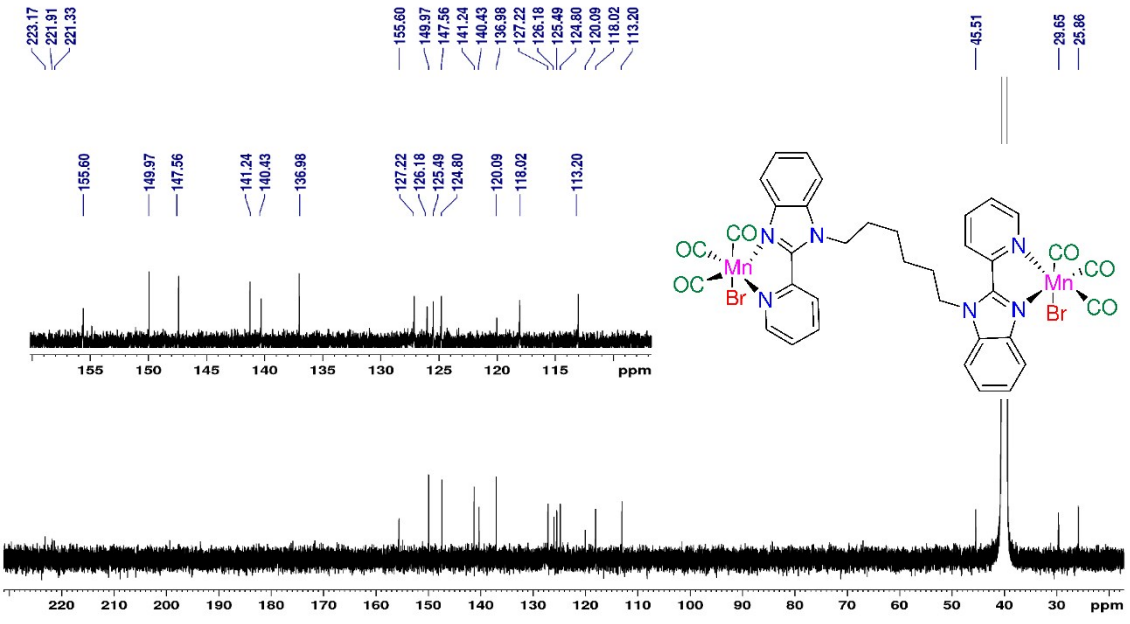
223.17
221.91
221.33
155.60
149.97
147.56
141.24
140.43
136.98
127.22
126.18
125.49
124.80
120.09
118.02
113.20
45.51
29.65
25.86
CO
OC
Mn
Br
N
ppm

(b)

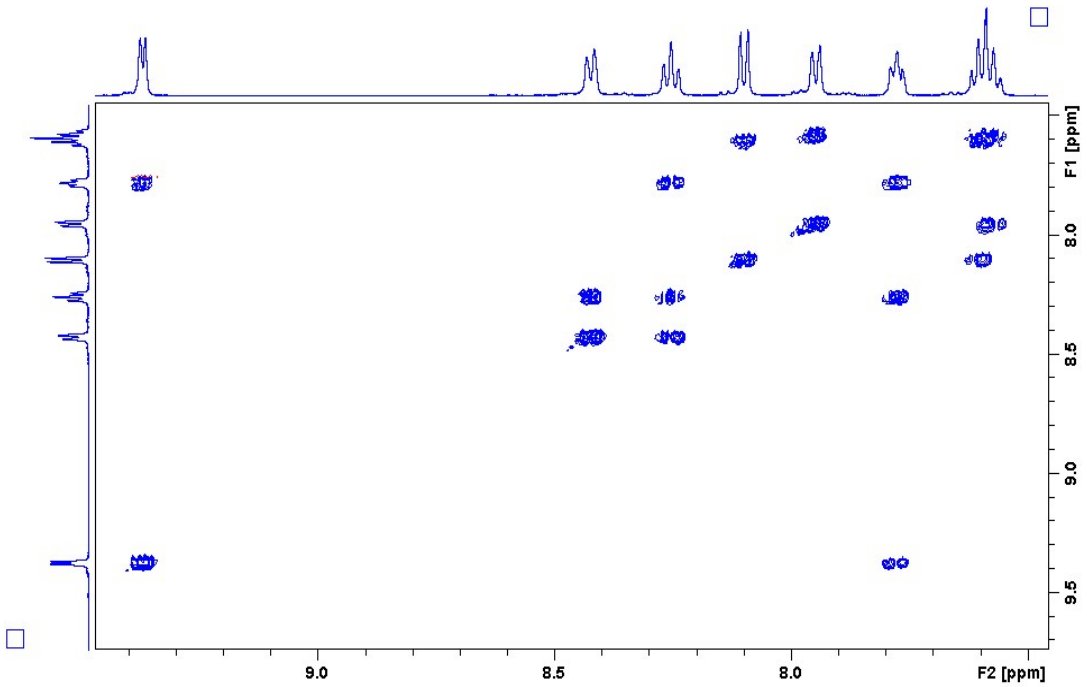

c)

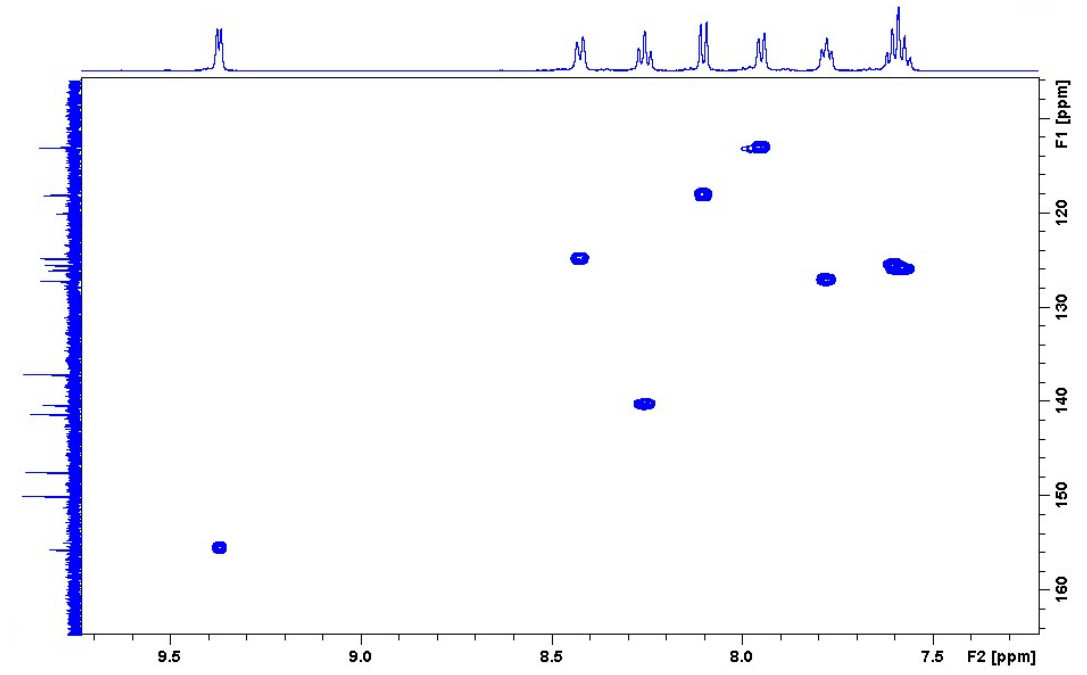

d)

Fig. S5: NMR analysis of **3** in DMSO-d_6, a) ^{1}H, b) ^{13}C, c) {^{1}H, ^{1}H} COS90, and d) {^{13}C, ^{1}H} HSQC.

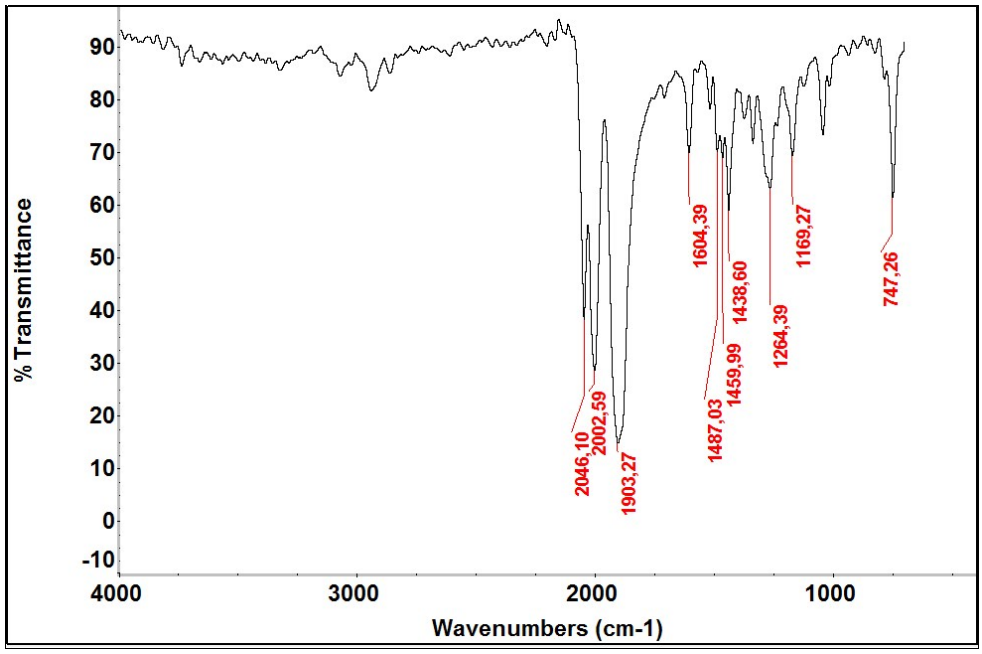

a)

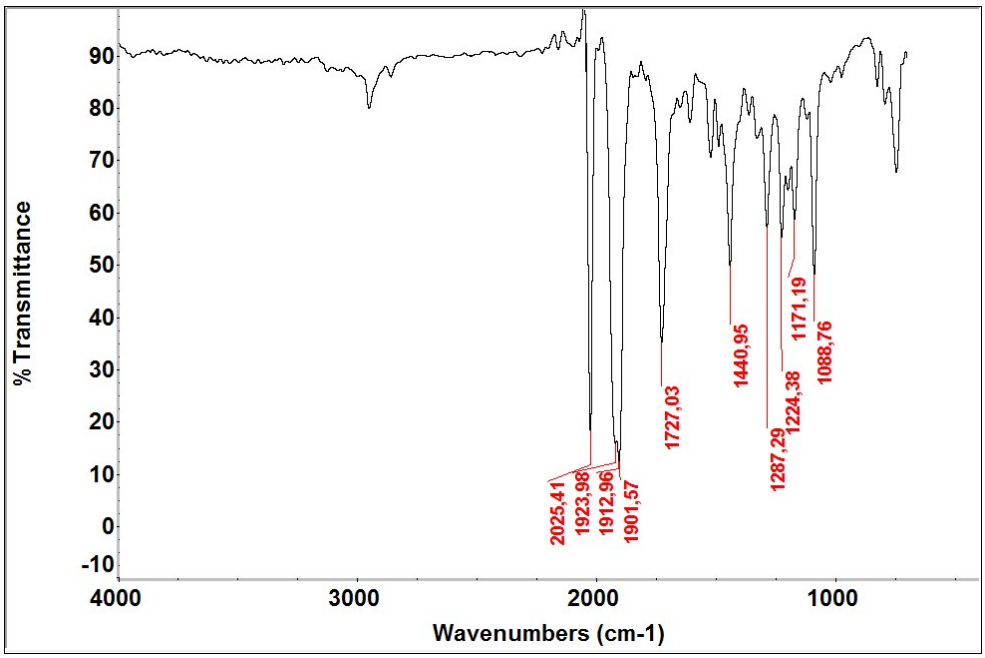

b)

Fig. S6: AT IR spectra of a) **4,** and b) **5**.

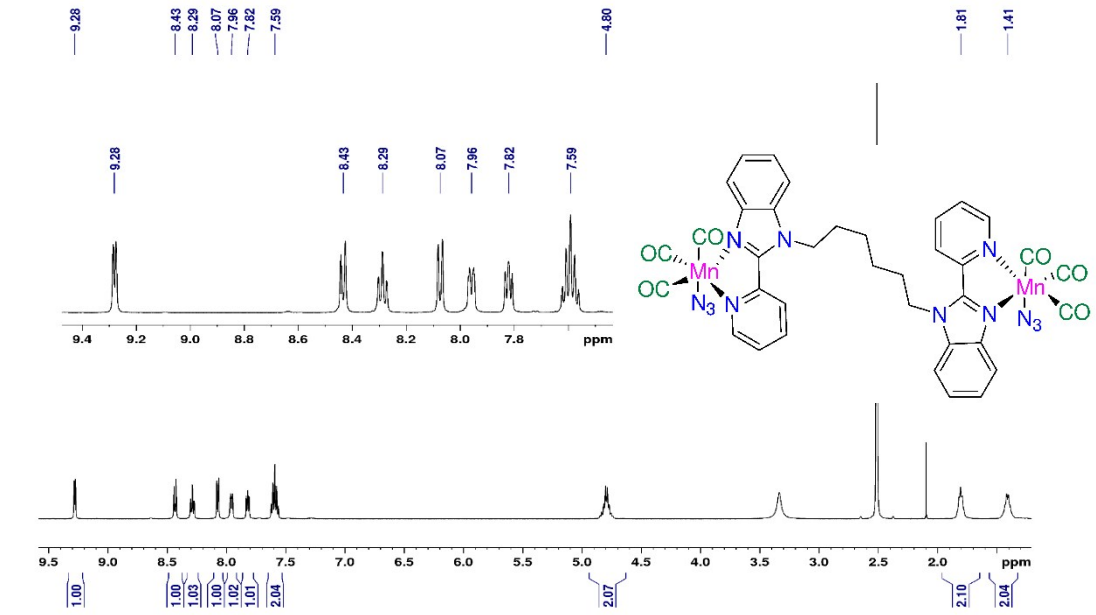

a)

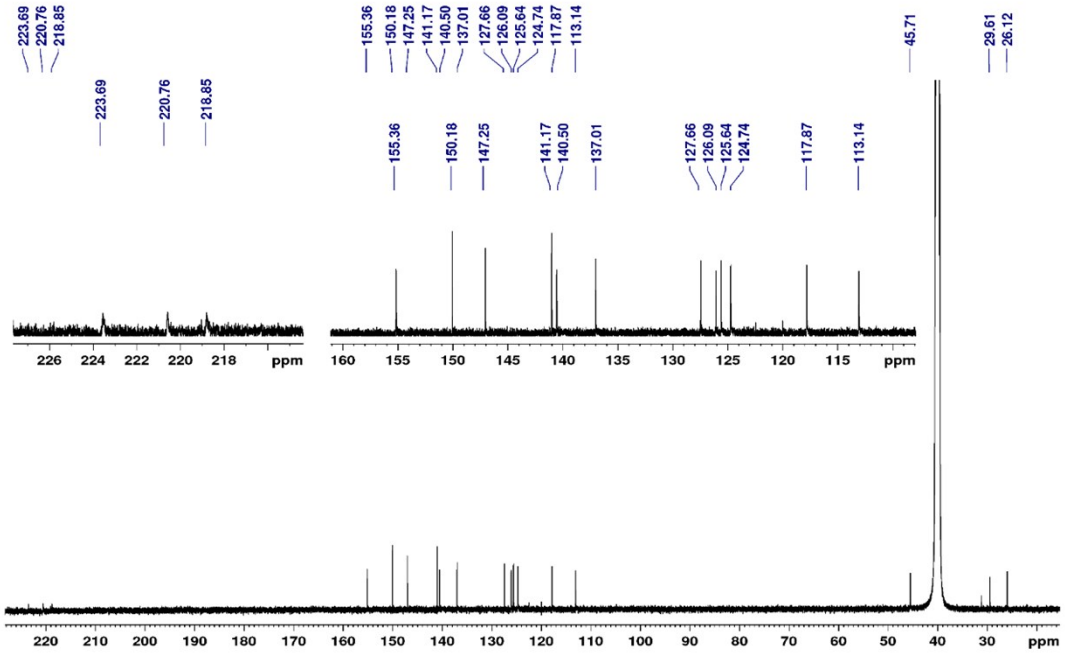

b)

Fig. S7: NMR analysis of **4** in DMSO-d_6, a) ^{1}H, and b) ^{13}C spectra.

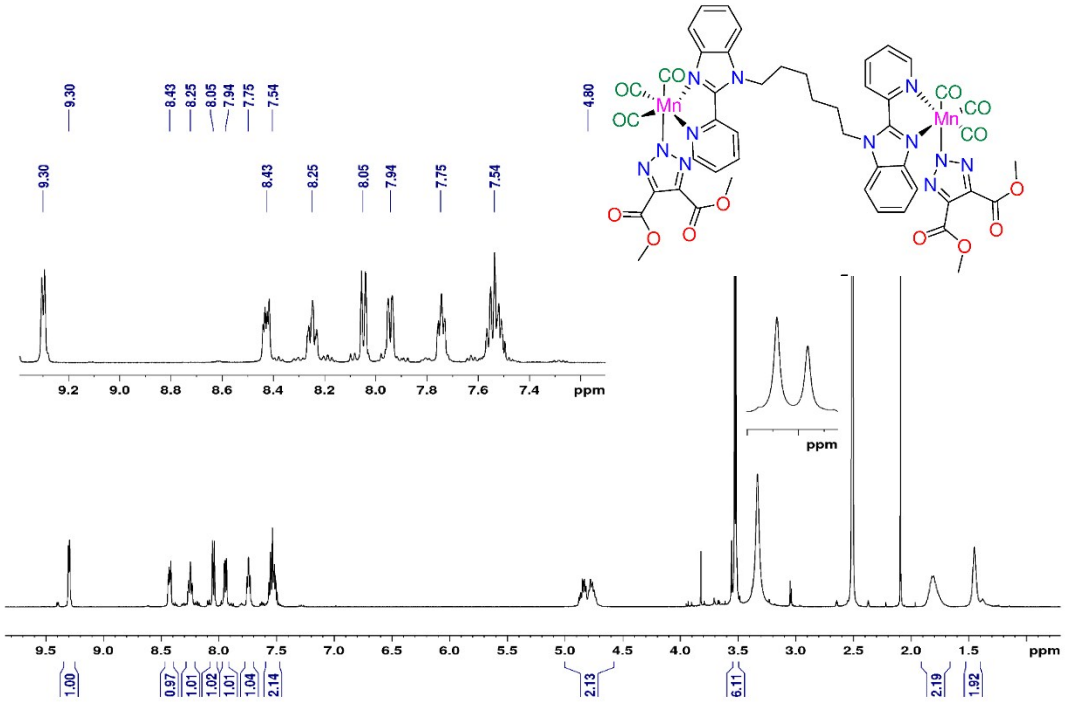

a)

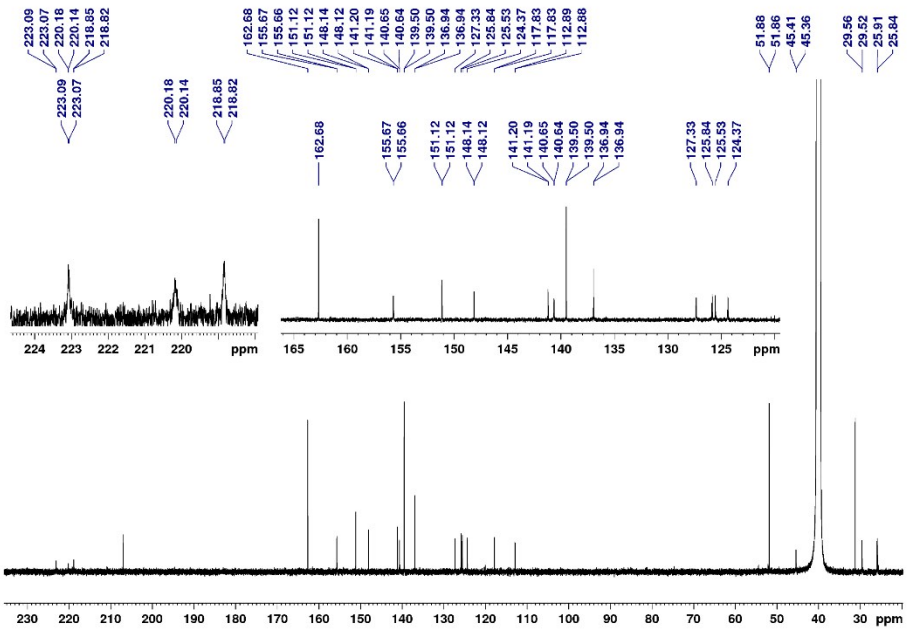

b)

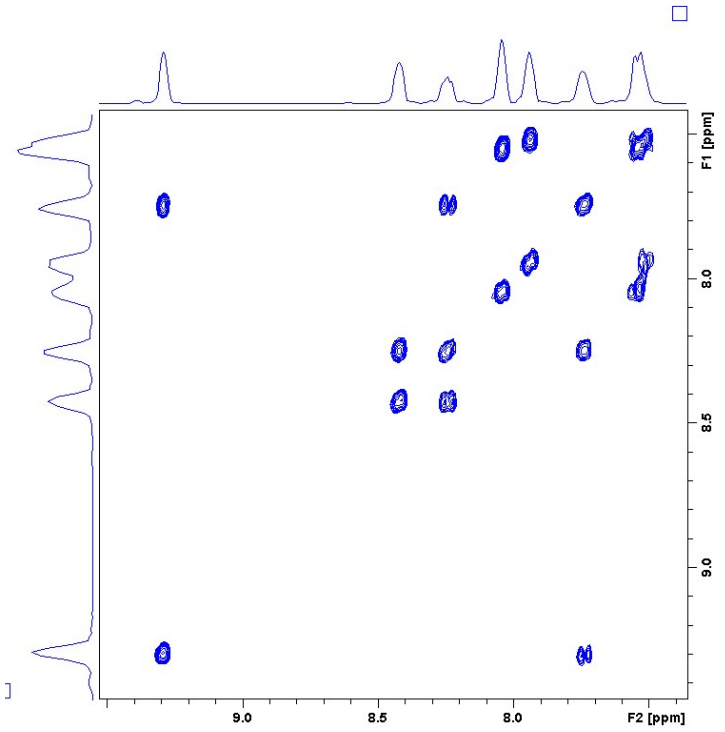

c)

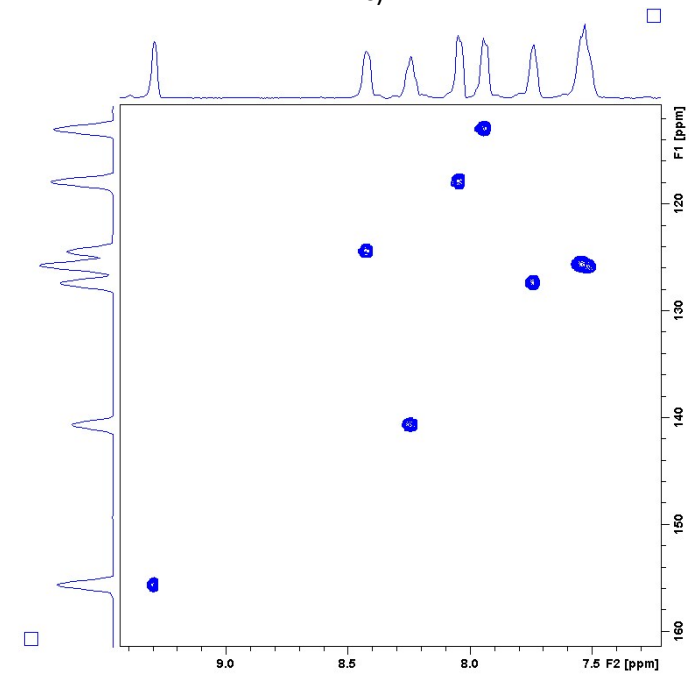

d)

Fig. S8: NMR analysis of **5** in DMSO-d_6, a) ^{1}H, b) ^{13}C, c) {^{1}H, ^{1}H} COS90, and d) {^{13}C, ^{1}H} HSQC.

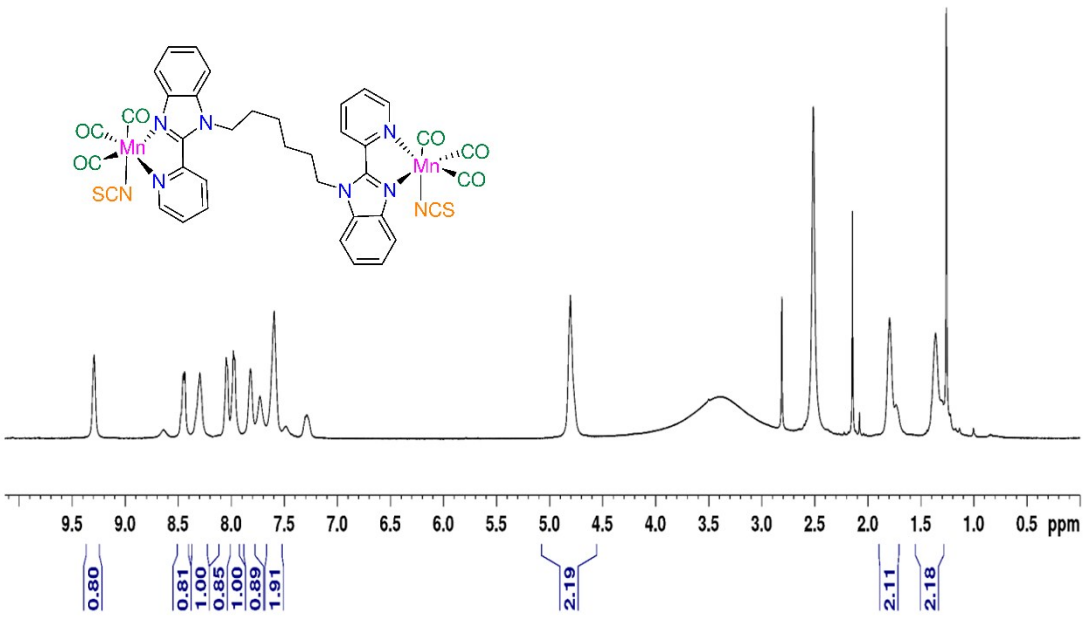
OC
CO
Mn
OC
SCN
N
N
N
N
CO
CO
Mn
CO
NCS
9.5 9.0 8.5 8.0 7.5 7.0 6.5 6.0 5.5 5.0 4.5 4.0 3.5 3.0 2.5 2.0 1.5 1.0 0.5 ppm
0.80
0.81
1.00
0.85
1.00
0.89
1.91
2.19
2.11
2.18

a)

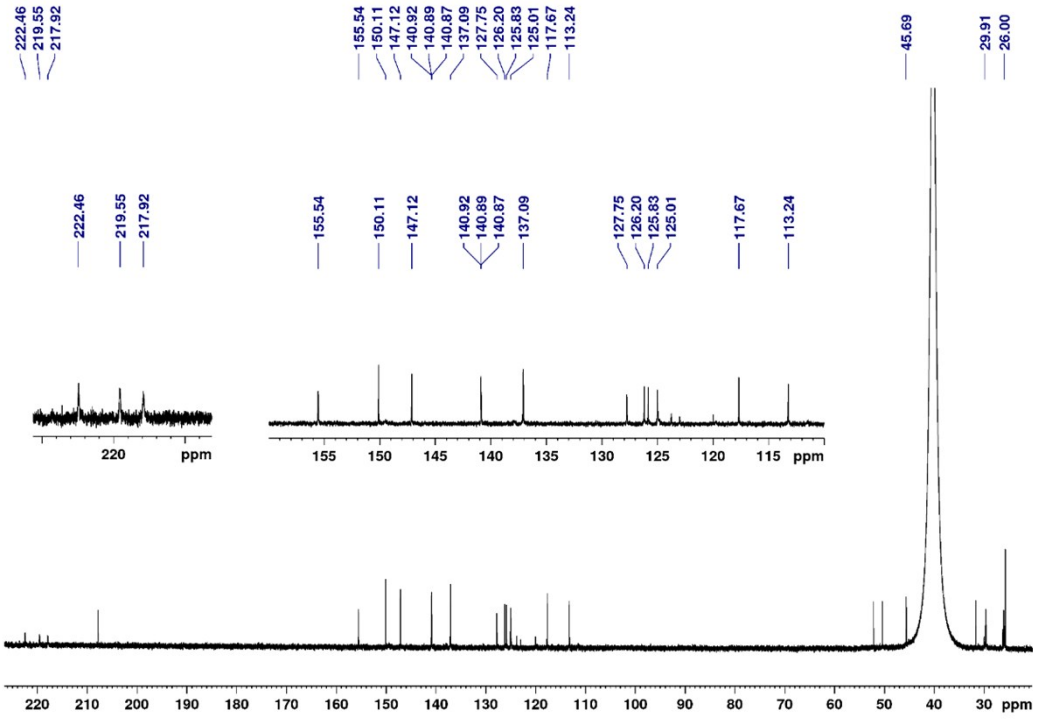
222.46
219.55
217.92
155.54
150.11
147.12
140.92
140.89
140.87
137.09
127.75
126.20
125.83
125.01
117.67
113.24
45.69
29.91
26.00
220 ppm
155 150 145 140 135 130 125 120 115 ppm
220 210 200 190 180 170 160 150 140 130 120 110 100 90 80 70 60 50 40 30 ppm

b)

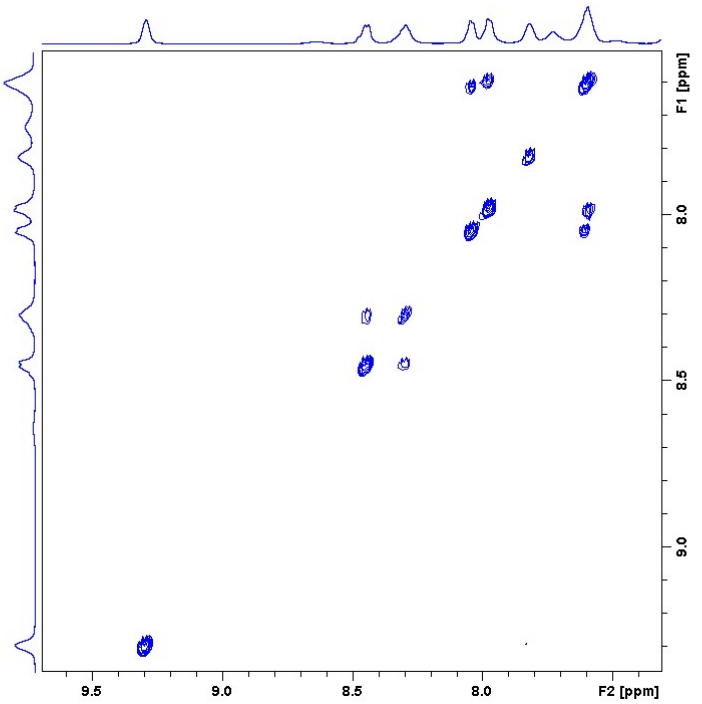

c)

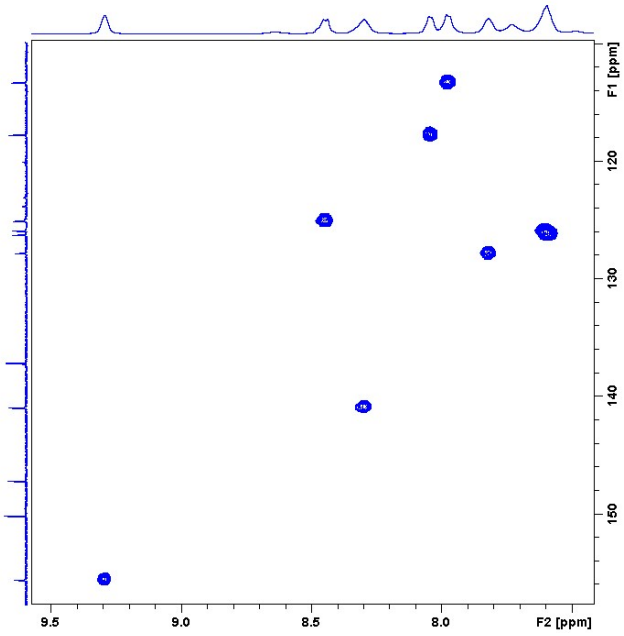

d)

Fig. S9: NMR analysis of **6** in DMSO-d_6, a) ^{1}H, b) ^{13}C, c) {^{1}H, ^{1}H} COS90, and d) {^{13}C, ^{1}H} HSQC.

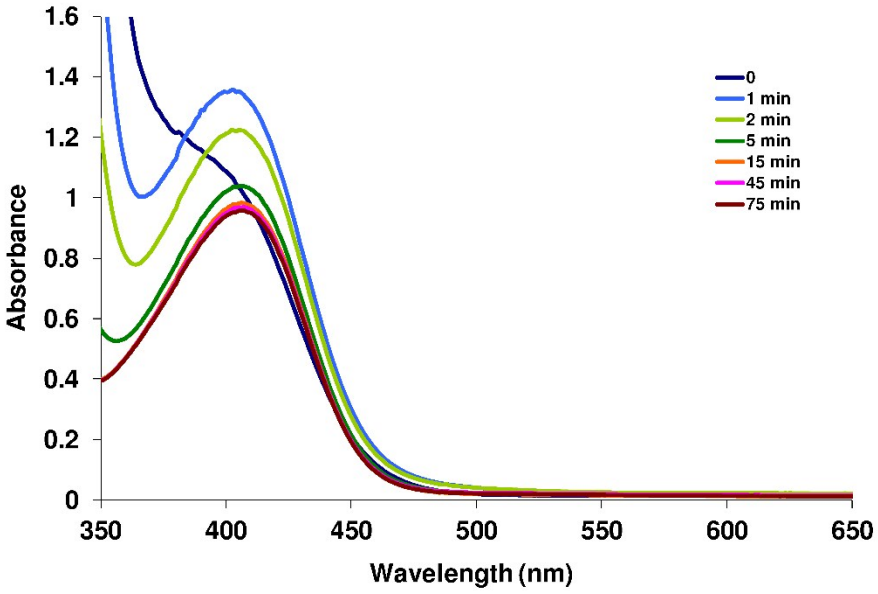
Absorbance
Wavelength (nm)
0
1 min
2 min
5 min
15 min
45 min
75 min

a)

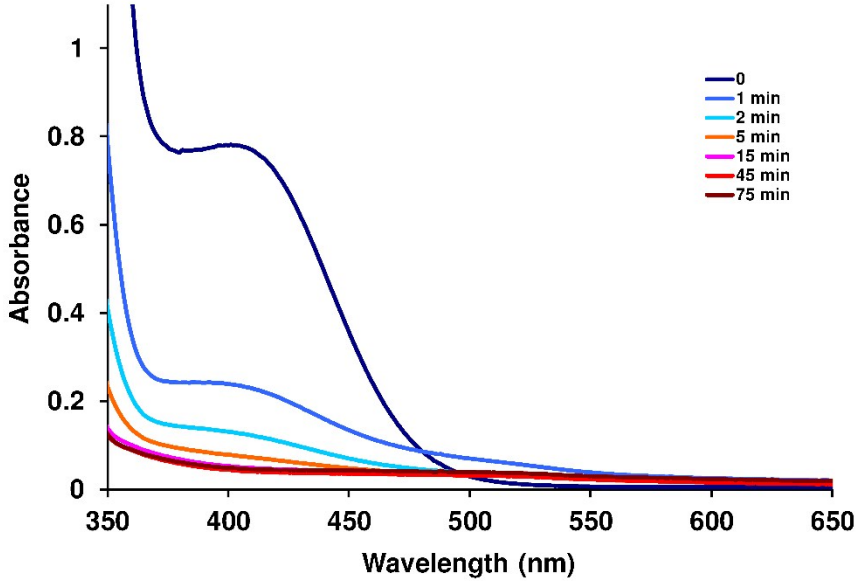
Absorbance
Wavelength (nm)
0
1 min
2 min
5 min
15 min
45 min
75 min

b)

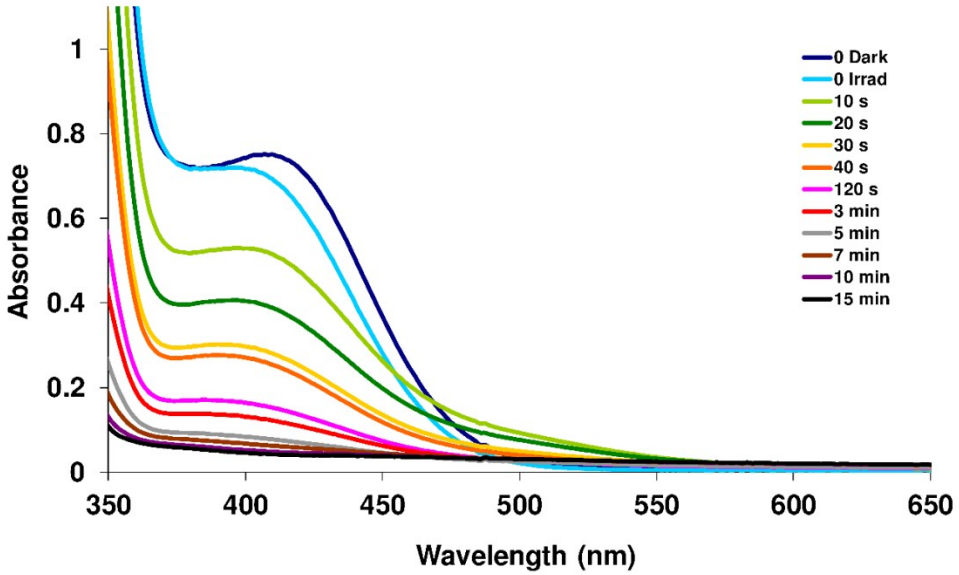

c)

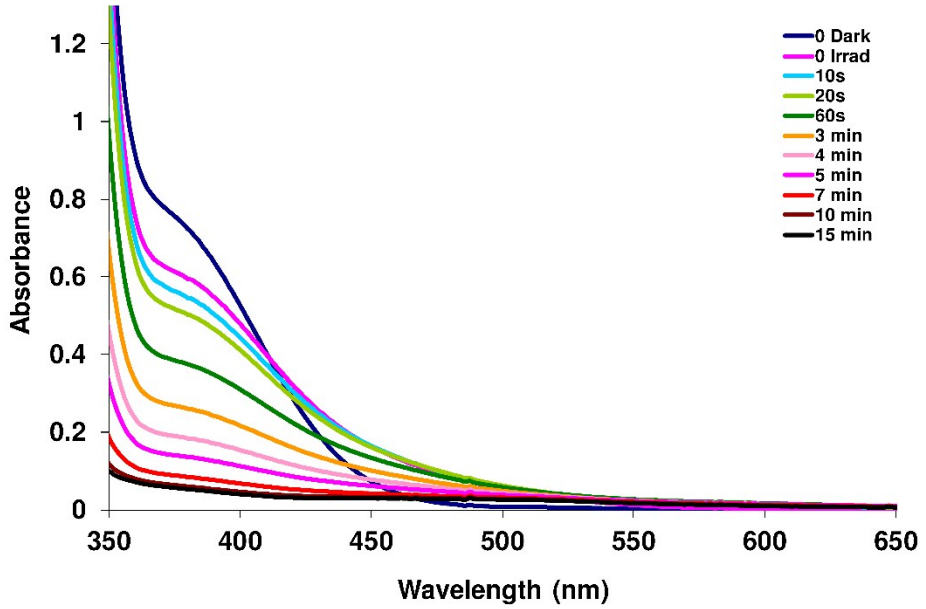

d)

Fig. S10: UV/Vis spectral changes of a) **1**, b) **2**, c) **3**, and d) **5** upon the photolysis at 468 nm for 0–15 min after pre-incubation in the dark for 16 h.

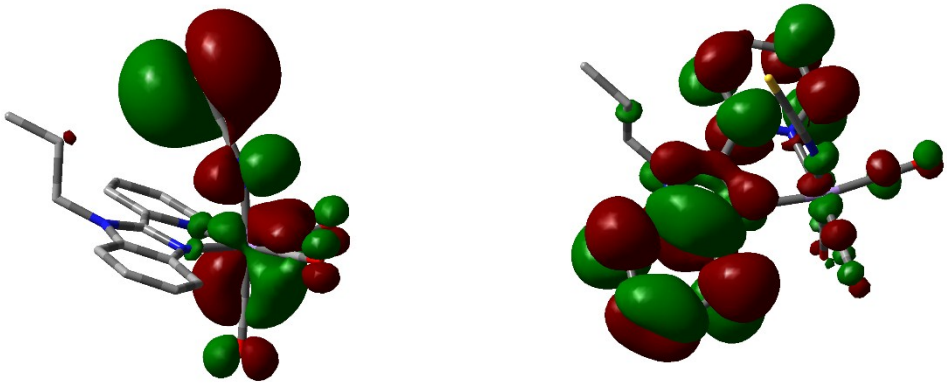

HOMO-1 LUMO+2

Fig. S11: FMO orbitals of the studied thiocyanate photoCORM **6**.

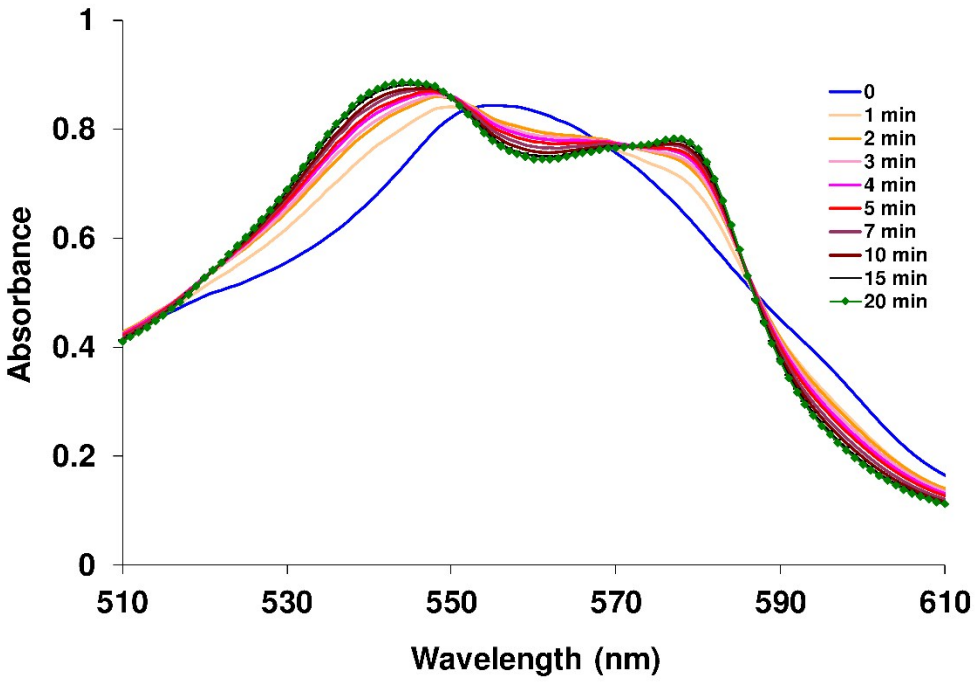

Fig. S12: UV/Vis spectral changes in the Q-band region of myoglobin (60 µM in 0.1 PBS at pH 7.4) with sodium dithionite (10 mM) and complex **3** (10 µM) under argon atmosphere upon photolysis (0–20 min) at 468 nm.

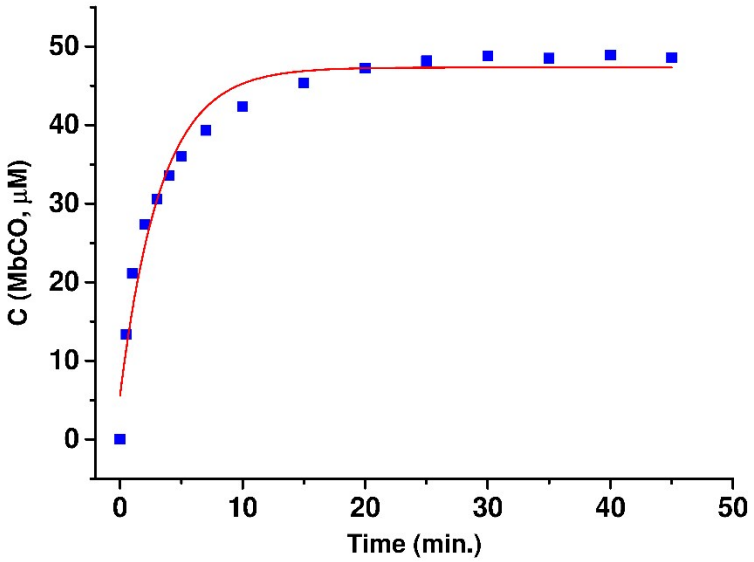
C (MbCO, μM)
Time (min.)
0
10
20
30
40
50

a)

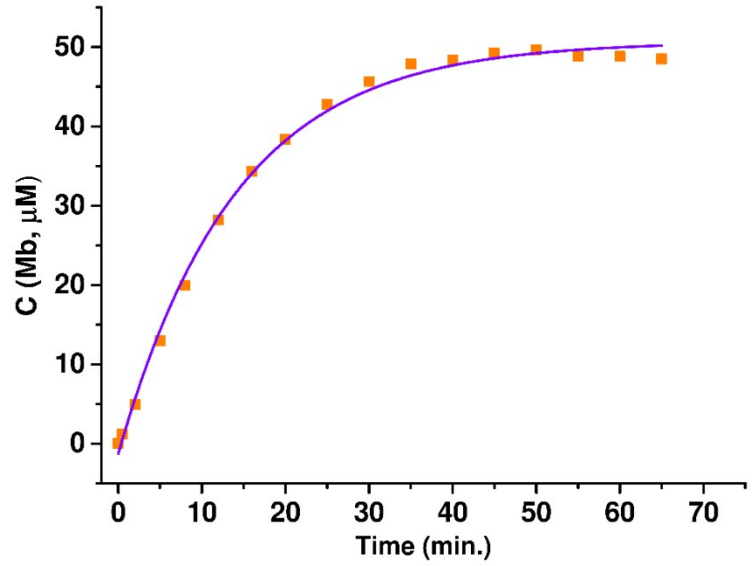
C (Mb, μM)
Time (min.)
0
10
20
30
40
50
60
70

b)

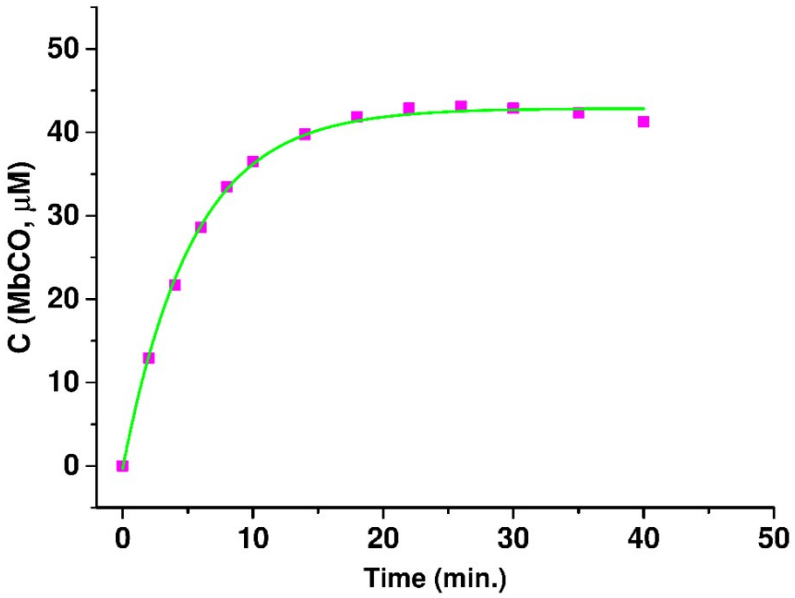

c)

Fig. S13: Relation between the concentration of MbCO (μM) and time (min.) upon the exposure of the myoglobin solution at 468 nm a) **3,** b) **5** and c) **6**.

Biological activity testing

Evaluation of antimicrobial properties

The antimicrobial activities of the benzimidazole ligands and their complexes were evaluated against cultures of *Staphylococcus aureus* ATCC 43300, *Escherichia coli* ATCC 25922, *Klebsiella pneumoniae* ATCC 700603, *Acinetobacter baumannii* ATCC 19606, *Pseudomonas aeruginosa* ATCC 27853, as well as two fungi, *Candida albicans* ATCC 90028 and *Cryptococcus neoformans var. grubii* H99; ATCC 208821. The samples were prepared in water (L^{SO3H}) and DMSO to a final testing concentration of 32 μg/mL and serially diluted 1:2 fold for 8 times. Each concentration was prepared in 384-well plates, non-binding surface plate (NBS; Corning 3640) for each bacterial/fungal strain, all in duplicate (n=2), and keeping the final DMSO concentration to a maximum of 0.5%. All bacteria were cultured in Cation-adjusted Mueller Hinton broth at 37 °C overnight. A sample of each culture was then diluted 40-fold in fresh broth and incubated at 37 °C for 1.5-3 h. The resultant mid-log phase cultures were diluted (CFU/mL, measured the absorbance at 600 nm), then added to each well of the compound containing plates, giving a cell density of 5×10^5 CFU/mL and a total volume of 50 μL. All the plates were covered and incubated at 37 °C for 18 h without shaking. The inhibition of the bacterial growth was determined by OD_{600} using a Tecan M1000 Pro monochromator plate reader. The percentage of growth inhibition was calculated for each well, using the negative control (media only) and positive control (bacteria without inhibitors) on the same plate as references. The MIC was determined as the lowest concentration at which the growth was fully inhibited, defined by an inhibition ≥ 80%. In addition, the maximal percentage of growth inhibition is reported as D_{Max}, indicating any compounds with partial activity plates.

Fungi strains were cultured for 3 days on Yeast Extract-peptone Dextrose agar at 30 °C. A yeast suspension of 1×10^6 to 5×10^6 CFU/mL (determined by OD_{600}) was prepared from five colonies. The suspension was subsequently diluted and added to each well of the sample-containing plates giving a cell density of fungi suspension of 2.5×10^3 CFU/mL and total volume of 50 μL. All plates were covered and incubated at 35 °C for 36 h without shaking. The growth inhibition of *Candida albicans* was measured at 630 nm, while that of *Cryptococcus neoformans* was determined by measuring the difference in absorbance at 600 and 570 nm, after the addition of resazurin (0.001%, final concentration) and incubation at 35 °C for 2 h. The absorbance was measured using a Biotek Multiflo Synergy HTX plate reader and controls. The MIC was determined as the lowest concentration at which the growth was fully inhibited, defined by an inhibition = 80% for *Candida albicans* and an inhibition = 70% for *Cryptococcus neoformans*. Due to a higher variance in the growth and inhibition, a lower threshold was applied to the data for *Cryptococcus neoformans*. In

addition, the maximal percentage of growth inhibition is reported as D_{Max}, indicating any compounds with marginal activity.